

# SCIENTIFIC REPORTS



OPEN

## A rapid and visual turn-off sensor for detecting copper (II) ion based on DNAzyme coupled with HCR-based HRP concatemers

Received: 14 October 2016

Accepted: 23 January 2017

Published: 07 March 2017

Wentao Xu<sup>1,2</sup>, Jingjing Tian<sup>2</sup>, Yunbo Luo<sup>1</sup>, Longjiao Zhu<sup>2</sup> & Kunlun Huang<sup>1,2</sup>

To solve the requirement of on-site, rapid, and visual detection of copper (II) ( $\text{Cu}^{2+}$ ) in aqueous solution, a turn-off sensor for detecting copper (II) ion was developed based on  $\text{Cu}^{2+}$ -dependent DNAzyme as the recognition element and hybridization chain reaction (HCR)-based horseradish peroxidase (HRP) concatemers as the signal amplifier and the signal report element. The detection unit, which was composed of the immobilized  $\text{Cu}^{2+}$ -dependent DNAzyme coupled with HCR-based HRP concatemers via Watson-Crick base pairing, could catalyze hydrogen peroxide ( $\text{H}_2\text{O}_2$ ) via TMB, generating obvious green color and turning yellow after sulfuric acid termination with optical absorption at 450 nm. Upon  $\text{Cu}^{2+}$  addition, the substrate strand of the  $\text{Cu}^{2+}$ -dependent DNAzyme concatenated with the HCR-based HRP complex was irreversibly cleaved, efficiently causing dramatic reduction of the detection signal. Under optimal conditions, the detection signal decreased with the concentration of  $\text{Cu}^{2+}$  in 5 min, exhibiting a linear calibration from 0.05 to 3  $\mu\text{M}$  with a detection limit of 8 nM. The sensor also displayed a high selectivity for  $\text{Cu}^{2+}$  given the specificity and anti-interference of the detection unit, and this system was applicable for monitoring  $\text{Cu}^{2+}$  in real water samples. Generally speaking, the proposed sensor exhibits good potential in environment surveys.

Heavy metal detection has received much attention in scientific research due to their serious threat to the environment and health<sup>1–4</sup>. Of particular interest there has been the detection of copper (II) ion, a dangerous pollutant that causes adverse afflictions in people upon excess intake, including liver or kidney damage, gastrointestinal disturbance<sup>5</sup>, Parkinson's disease, Wilson's disease and Alzheimer's disease<sup>3,4</sup>. Considering its toxicity, the Chinese Ministry of Health (CMH), U.S. Environment Protection Agency (EPA) and World Health Organization (WHO) regulate maximum permissible levels of copper (II) of less than 15  $\mu\text{M}$ <sup>6</sup>, 20  $\mu\text{M}$ <sup>7</sup> and 31  $\mu\text{M}$  in water<sup>8</sup>, respectively. Thus, instrumental analytical techniques for  $\text{Cu}^{2+}$  detection have been developed, such as inductively coupled plasma mass spectrometry (ICP-MS)<sup>9</sup>, atomic absorption spectrometry (AAS)<sup>10</sup>, inductively coupled plasma atomic emission spectrometry (ICP-OES) and fluorescence spectrometry<sup>11,12</sup>. However, these widely used instrumental techniques are rather complicated, requiring sophisticated apparatus and professional personnel, which are obstructive to further application. To keep pace with expectations in future on-site rapid testing, the development of new sensing techniques for  $\text{Cu}^{2+}$  is a hot issue in analytical chemistry in recent years.

Among numerous new sensors, DNAzyme-based biosensors are of particular interest<sup>13,14</sup>. DNAzyme, a type of functional nucleic acid, is able to catalyze a series of reactions. Recently, two types of DNAzyme have been a hot topic of research. One type of DNAzyme is G-quadruplex-based DNAzyme, which possesses mimic-horse radish peroxidase (HRP) activity to catalyze specific substrate for chromogenic reaction<sup>15–19</sup>. The other type is metal ion-dependent DNAzyme, which could depend on specific metal ions as cofactors, such as  $\text{Ag}^+$  ions<sup>20</sup>,  $\text{Na}^+$  ions<sup>21,22</sup>,  $\text{Cu}^{2+}$  ions<sup>23–25</sup>,  $\text{Pb}^{2+}$  ions<sup>26,27</sup>,  $\text{Mg}^{2+}$  ions<sup>28</sup>,  $\text{Zn}^{2+}$  ions<sup>29,30</sup>,  $\text{Ca}^{2+}$  ions<sup>31,32</sup>,  $\text{Cd}^{2+}$  ions<sup>33</sup>,  $\text{UO}_2^{2+}$  ions,  $\text{Hg}^{2+}$  ions<sup>34,35</sup>, and lanthanide ions<sup>36–38</sup>. Most metal ions activate specific DNAzyme via cleavage. According to the nucleotide type of cleavage site (ribonucleotide and deoxyribonucleotide), metal ion-dependent DNAzyme classified as RNA-cleaving DNAzyme and DNA-cleaving DNAzyme.  $\text{Cu}^{2+}$ -specific DNAzyme, which belongs

<sup>1</sup>Beijing Advanced Innovation Center for Food Nutrition and Human Health, College of Food Science & Nutritional Engineering, China Agricultural University, Beijing 100083, China. <sup>2</sup>Beijing Laboratory for Food Quality and Safety, College of Food Science and Nutritional Engineering, China Agricultural University, Beijing 100083, China. Correspondence and requests for materials should be addressed to K.H. (email: foodsafety66@cau.edu.cn)

to DNA-cleaving DNAzyme with the characteristics of easy synthesis, lower cost and better stability, leads to site-specific cleavage at the guanine position of the substrate in catalytic/substrate multiple strands, which makes it an ideal element for  $\text{Cu}^{2+}$  ion detection due to inherent advantages of outstanding stability under harsh conditions and high selectivity comparable to antibodies<sup>14,39,40</sup>. Over the past decade, different DNAzyme-based biosensors for  $\text{Cu}^{2+}$  using various signal transduction methods have been developed, including fluorescence<sup>41,42</sup>, colorimetry<sup>39,42–44</sup> and lateral flow nucleic acid techniques<sup>45</sup>. Such DNAzyme-based sensing strategies require simpler apparatus and less professional personnel than traditional techniques.

Interestingly, hybridization chain reactions (HCR), which generate linear DNA nanostructures arisen by self-assembly of short DNA fragments through a cross-opening process, have recently become one of the most active research areas in molecular biology and DNA diagnostics relying on several unique advantages<sup>46,47</sup>. Firstly, signal amplification via Watson-Crick base pairing is easier to achieve, which can lead to ultrasensitive detections. Secondly, HCR exhibit the potential of signal reporting via special labels, which pave the way toward multi-target sensing platforms. However, HCR rely on reaction time and are temperature-dependent, so a relatively long time or appropriate temperature likely triggers false positives that interfere with the results. In our research, the HCR was prepared in advance via ingenious hairpin design, effectively eliminating undesirable initiation. Herein, we achieved the proof-of-concept to integrate  $\text{Cu}^{2+}$ -dependent DNAzyme with HCR-based HRP concatemers for rapid detection of  $\text{Cu}^{2+}$  semi-quantitatively observed by the naked eye and quantitatively monitored by a portable spectrophotometer in 5 min, exhibiting immense potential for on-site detection.

## Experiment Section

**Reagents and Apparatus.** All oligonucleotides were HPLC-purified and synthesized at Invitrogen (Life Technologies, Beijing, China). The substrate strand and catalytic strand for copper (II)-dependent DNAzyme were designed according to the literature<sup>42</sup>. The sequences of the oligonucleotides are as follows:

Substrate strand for  $\text{Cu}^{2+}$ -dependent DNAzyme ( $S_1$ ):  
 5'-GGGGGGGGGGGGGGGGGGGGGGGGGTTTTTTTAGCTTCTTTCTAATACGGCTTACCTT  
 TTTTTTTT-Biotin-3'  
 Catalytic strand for  $\text{Cu}^{2+}$ -dependent DNAzyme ( $S_2$ ):  
 5'-GGTAAGCCTGGGCCTCTTTCTTTTTAAGAAAGAAC-3'  
 Linker-labeled initiator ( $S_3$ ):  
 5'-CTGAGCTTCGGATTCTGTTTGGCCCCCCCCCCCCCCCCCCCC-3'  
 Hairpin DNA ( $H_1$ ):  
 5'-Biotin-GGCCAAACAGAATCCGAAGCTCAGACCCTGCTGAGCTTCGGATTCTGT-3'  
 Hairpin DNA ( $H_2$ ):  
 5'-Biotin-CTGAGCTTCGGATTCTGTTTGGCCACAGAATCCGAAGCTCAGCAGGGT-3'

The ingenious design of hairpins should meet the following requirements: Hairpins ( $H_1$  and  $H_2$ ) should possess the same number of bases and the same number of sticky ends. Noticeably, the sticky ends of  $H_1$  locates at the 5'-end while that of  $H_2$  locates at the 3'-end. To better promote HCR, nearly half fragment of  $H_2$  at the 5'-end was truncated as the initiator strand. High binding polystyrene 96-well microplate was purchased from Costar (NY, USA). In addition, 4-(2-hydroxyethyl) piperazine-1-ethanesulfonic acid (HEPES), ascorbate, streptavidin (SA), bovine serum albumin (BSA), and streptavidin-horseradish peroxidase (SA-HRP) were obtained from Sigma-Aldrich Chemical Co. (St. Louis, MO, USA). Tetramethylbenzidine (TMB) coloring solution was purchased from Biyuntian Co. Ltd (Beijing, China). Ultrapure water was used throughout the experiment and was obtained from a Milli-Q water purifying system (resistivity  $\geq 18.2 \text{ M}\Omega \text{ cm}^{-1}$ , Milli-Q, Millipore). Other chemicals were of analytical grade and were used without further purification.

Gel electrophoresis was conducted on a Molecular Imager Gel Doc XR (Bio-Rad, Canada). Visual measurements were carried out with a portable spectrophotometer (NS810, Shenzhen 3nh Technology Co., Ltd). The transmission electron micrograph (TEM) was performed on a JEOL JEM-1400 Transmission electron micrograph (Germany).

**Immobilization of copper (II)-dependent DNAzyme.** To immobilize  $\text{Cu}^{2+}$ -dependent DNAzyme,  $2 \mu\text{g}/\text{mL}$  SA ( $100 \mu\text{L}$ ) in carbonate buffer solution (CBS,  $15 \text{ mM Na}_2\text{CO}_3$ ,  $35 \text{ mM NaHCO}_3$ , pH 9.6) was added to wells and incubated at  $37^\circ\text{C}$  for 2 h. After washing three times with  $250 \mu\text{L}$  wash buffer ( $0.15 \text{ M NaCl}$ ,  $10 \text{ mM K}_2\text{HPO}_4$ ,  $1 \text{ mM NaH}_2\text{PO}_4$ ,  $0.05\%$  Tween 20, pH 7.4), the wells were blocked with  $200 \mu\text{L}$  of  $1\%$  BSA per well at  $37^\circ\text{C}$  for 2 h. Then,  $100 \mu\text{L}$  biotinylated  $S_1$  ( $120 \text{ nM}$ ) dissolved in phosphate buffer solution (PBS,  $0.15 \text{ M NaCl}$ ,  $10 \text{ mM K}_2\text{HPO}_4$ ,  $1 \text{ mM NaH}_2\text{PO}_4$ , pH 7.4) was added to each well of 96-well plates and incubated at  $37^\circ\text{C}$  for 1 h. Next, the wells were washed three times with wash buffer, incubated with  $S_2$  ( $150 \text{ nM}$ ) dissolved in  $50 \text{ mM}$  HEPES buffer (pH 7.0) containing  $1.5 \text{ M NaCl}$  at  $37^\circ\text{C}$  for 100 min and washed three times again.

**Preparation of HCR-based HRP concatemers.** Biotinylated hairpins ( $H_1$  and  $H_2$ ) were heated at  $95^\circ\text{C}$  for 5 min and then cooled to  $4^\circ\text{C}$  slowly for 1.5 h before use. The hybridization chain reaction (HCR) proceeded at  $37^\circ\text{C}$  for 1 h, composed of  $200 \text{ nM}$   $S_3$ ,  $1 \mu\text{M}$   $H_1$  and  $1 \mu\text{M}$   $H_2$  in Tris-HCl Buffer ( $10 \text{ mM}$  Tris,  $500 \text{ mM NaCl}$ ,  $1 \text{ mM MgCl}_2$ , pH 7.4). Afterwards, SA-HRP ( $500 \text{ ng}/\text{mL}$ ) was added to the HCR system and incubated at  $37^\circ\text{C}$  for 1 h to form the HCR-HRP complex. HCR products were detected by  $2\%$  EB-stained agarose gel electrophoresis. HCR-based HRP concatemers was inspected by the transmission electron micrograph<sup>48</sup>.

**Assembly of the detection unit and copper (II) assay.** Immobilized  $\text{Cu}^{2+}$ -dependent DNAzyme was concatenated with HCR-based HRP complex ( $100 \mu\text{L}$ ) in each well at  $37^\circ\text{C}$  for 2 h. After washing three times,

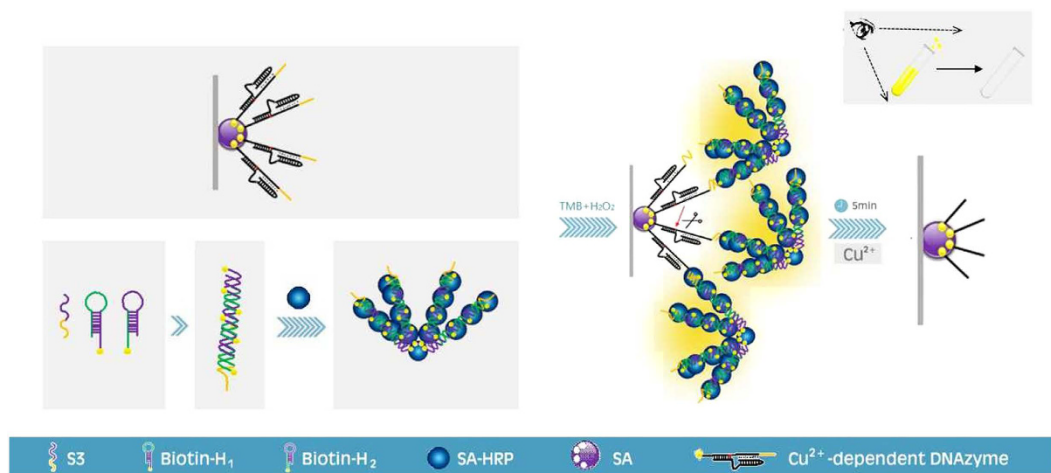


**Figure 1.** Schematic of the design of the turn-off sensor for the detection of copper (II) ion ( $\text{Cu}^{2+}$ ) based on  $\text{Cu}^{2+}$ -dependent DNAzyme coupled with HCR-based HRP concatemers.

the detection unit of  $\text{Cu}^{2+}$  was achieved. Then a fixed concentration of  $\text{Cu}^{2+}$  ( $\text{CuSO}_4$ ,  $100 \mu\text{L}$ ) dispersed in the reaction buffer (1.5 M NaCl, 50 mM HEPES and  $50 \mu\text{M}$  ascorbate) was incubated with the  $\text{Cu}^{2+}$ -detection unit in each well at  $37^\circ\text{C}$  for 5 min. The same volume of reaction buffer was used as the negative control. After washing three times,  $100 \mu\text{L}$  TMB coloring solution was added to each well. Then, the samples were incubated at room temperature away from light for 5 min, and  $50 \mu\text{L}$   $\text{H}_2\text{SO}_4$  (2 M) was added to terminate the chromogenic reaction. The absorbance values at 450 nm ( $\text{OD}_{450}$ ) were monitored by a portable spectrophotometer.

**HPLC-DAD analysis.** Conditions for DNA analysis followed the description by Wilde *et al.* with some modifications<sup>49</sup>. HPLC analyses were performed on an Agilent 1100 HPLC system together with a diode array detector (DAD). A TSKgel DNA-NPR (4.6 mm i.d.  $\times$  7.5 cm, Tosoh, Japan) was employed. DNA samples were separated by buffer A (20 mM Tris, pH 9.0) and buffer B (1 M NaCl in 20 mM Tris, pH 9.0) according to the following gradient: 25–45% B in 0–0.13 min, 45–50% B in 0.13–4 min, 50–64% B in 4–25 min, 25% B in 25.1–35 min. The flow rate was 0.4 mL/min with an injection volume of  $10 \mu\text{L}$ . DNA elution was monitored by UV absorbance at 260 nm. All chromatography was performed at  $35^\circ\text{C}$ .

**Detection of real water samples.** Non-contaminated commercial bottled purified water was purchased from the local supermarket. Lake water was collected from Beijing Olympic Green Park, Beijing, China. Domestic sewage was obtained from the Beijing north river sewage treatment factory, Chaoyang District, Beijing, China. Firstly, the water samples were gently mixed with  $\text{Cu}^{2+}$  standard solution, generating two final  $\text{Cu}^{2+}$  concentrations ( $0.5 \mu\text{M}$  and  $2.5 \mu\text{M}$ ). Then, a  $90\text{-}\mu\text{L}$  water sample was mixed with  $10 \mu\text{L}$   $10\times$  reaction buffer (15 M NaCl, 500 mM HEPES and  $500 \mu\text{M}$  ascorbate), and the obtained  $100\text{-}\mu\text{L}$  solution was treated using the same protocol as noted above for the  $\text{Cu}^{2+}$  detection. The ICP-MS analysis for  $\text{Cu}^{2+}$  in real water samples was based on Szpunar's study<sup>6</sup>.

## Result and Discussion

**Design principle of turn-off sensor.** The rapid and visual DNA concatenation sensor for  $\text{Cu}^{2+}$  detection is schematically illustrated in Fig. 1. Beforehand, SA was immobilized onto the high binding polystyrene well via hydrophobic effect. Then,  $S_1$  was captured via biotin-streptavidin combination, which was flanked with spacer sequences of poly-thymine (poly-T) oligonucleotides at the 3' end and with linker sequence of poly-guanine (poly-G) oligonucleotides at the 5' end. Via Watson-Crick base pairing at the 3' terminus and the formation of the DNA triplex at the 5' terminus,  $S_2$  coupling with  $S_1$  formed the  $\text{Cu}^{2+}$ -dependent DNAzyme. So  $\text{Cu}^{2+}$ -dependent DNAzyme was coated onto the well via biotin-streptavidin linkage to identify the target.

Simultaneously, SA-HRP and the nicked DNA double-helix formed a complex. In the presence of linker-labeled initiator, biotinylated hairpin 1 ( $H_1$ ) first underwent an unbiased strand-displacement reaction to open the hairpin from the 5' sticky end. The newly exposed sticky nucleates of  $H_1$  opened biotinylated hairpin 2 ( $H_2$ ) and underwent a strand-displacement reaction, exposing another sticky end. Similarly, a chain reaction of hybridization events was propagated to form the biotinylated nicked DNA double-helix, acting as the signal amplifier. In the presence of SA-HRP, which often served as the signal output element, the linker-labeled HCR-based HRP complex formed via biotin-streptavidin linkage. Given that HCR-based HRP complex not only amplified detection signal but also catalyzed hydrogen peroxide ( $\text{H}_2\text{O}_2$ ) via TMB, generating obvious yellow color visible to the naked eye and optical intensity at 450 nm ( $\text{OD}_{450}$ ) after sulfuric acid termination, the HCR-based HRP complex acted as a signal amplification element as well as a signal report element.

Finally,  $\text{Cu}^{2+}$ -dependent DNAzyme concatenated with the HCR-based HRP complex was achieved via Watson-Crick base pairing. Upon target  $\text{Cu}^{2+}$  introduction,  $S_1$  of the  $\text{Cu}^{2+}$ -dependent DNAzyme concatenated with the HCR-based HRP complex was irreversibly cleaved. We hypothesized that the cleaved pieces were released and totally washed, leading to the dramatic reduction in  $\text{OD}_{450}$  values and absence of yellow color.

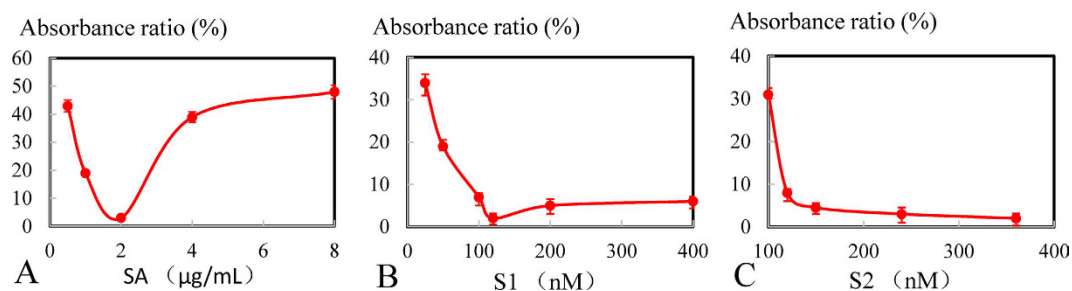


**Figure 2. Optimization of immobilized  $\text{Cu}^{2+}$ -dependent DNAzyme.** (A) Absorbance ratio (%) of the turn-off sensor with different concentrations of SA ( $\mu\text{g}/\text{mL}$ ). The concentrations from the left are 0.5, 1, 2, 3, and  $8\ \mu\text{g}/\text{mL}$ . (B) Absorbance ratio (%) of the turn-off sensor with different concentrations of  $S_1$  (nM). The concentrations from the left are 25, 50, 100, 120, 200, and 400 nM. (C) Absorbance ratio (%) of the turn-off sensor with different concentrations of  $S_2$  (nM). The concentrations from the left are 100, 120, 150, 240, and 360 nM. Error bars represent standard deviation ( $N = 3$ ).

**Optimization of the immobilized  $\text{Cu}^{2+}$ -dependent DNAzyme.** Given that the  $\text{Cu}^{2+}$ -dependent DNAzyme was immobilized onto the surface via biotin-streptavidin linkage, the concentrations of SA, biotinylated substrate strand ( $S_1$ ) and  $\text{Cu}^{2+}$  catalytic strand ( $S_2$ ) were optimized. As illustrated in Fig. 2, the following equation was employed: absorbance ratio (%) =  $A_0/A \times 100$  at  $450\ \text{nm}$ <sup>7</sup>, where  $A_0$  and  $A$  represent the optical intensity after and before  $\text{Cu}^{2+}$  sample addition, respectively. Smaller the ratio, more remarkable the signal variation was, indicating the more appropriate detection conditions. In Fig. 2A, with the SA concentration ranging from 0.5 to  $8\ \mu\text{g}/\text{mL}$ , the absorbance ratio (%) exhibited a wave trough and a valley point at  $2\ \mu\text{g}/\text{mL}$  of SA, presumably due to stereo-hindrance effects. Small amounts of SA could not capture sufficient amounts of the biotinylated substrate strand, whereas excess SA would lead to steric hindrance, reducing binding with the strand<sup>50</sup>. In Fig. 2B, the ratio gradually declined until reaching a plateau at 120 nM from low dose to high dose, mainly because the combination of streptavidin with biotin conformed to the molar ratio of one to four (SA:  $2\ \mu\text{g}/\text{mL} \approx 30\ \text{nM}$ )<sup>51,52</sup>. In Fig. 2C, the ratio was reduced from 100 to 150 nM and subsequently maintained a relatively low value, indicating that slightly excessive  $S_2$  compared with  $S_1$  was ideal for saving experimental materials. In general,  $2\ \mu\text{g}/\text{mL}$  of SA, 120 nM of  $S_1$  and 150 nM of  $S_2$  were optimal.

**Characterization of the Chromatographic Behavior of the  $\text{Cu}^{2+}$ -dependent DNAzyme on a DNA-NPR Column.** Anion exchange chromatography is a widely used technique for separating negatively-charged DNA molecules. The TSK gel DNA-NPR column is a polymer-based anion exchange column for improved DNA resolution over a wide molecular weight range. The capability of the TSK gel DNA-NPR column to separate both high and low molecular weight DNA fragments has been demonstrated by Wilde *et al.*<sup>49</sup>. Figure 3A,B and C present typical elution profiles of the negative control of the reaction buffer, before and after the  $\text{Cu}^{2+}$  cleavage of the  $\text{Cu}^{2+}$ -dependent DNAzyme, respectively. In Fig. 3A, the negative control showed a high response value at the retention time of 1.187 min with the corresponding peak area of 917. Compared with the negative control, Fig. 3B revealed a relatively high response value at the retention time of 19.835 min with the corresponding peak area of 3073, indicating that the chromatographic peak resulted from the non-dissected  $\text{Cu}^{2+}$ -dependent DNAzyme. In Fig. 3C, there was no response at 19.835 min, whereas a new high chromatographic peak appeared at the retention time of 9.239 min compared with Fig. 3B, suggesting the split  $\text{Cu}^{2+}$ -dependent DNAzyme. Based on these scientific data, we concluded that the  $\text{Cu}^{2+}$ -dependent DNAzyme was cut into small pieces after  $\text{Cu}^{2+}$  sample addition.

**Optimization of HCR-based HRP concatemers.** As the signal amplifier and signal report element, HCR-based HRP concatemers were optimized, including HCR and the dosage of SA-HRP. To the best of our knowledge, the signal amplification effect of HCR depends on the length of the hybridization chain. Longer the HCR product, the better the effect of signal amplification is. Inspiringly, the longitude of the hybridization chain was hinged on the ratio between the dose of the initiator and two closed hairpins<sup>53</sup>. As proof-of-principle (Fig. 4A), the HCR between the initiator ( $S_3$ ) and  $H_1$  and  $H_2$  was examined by agarose gel electrophoresis. In the absence of  $S_3$ , a bright band of  $H_1$  (lane 2) and  $H_2$  (lane 3) could be observed, and the HCR between  $H_1$  and  $H_2$  was inhibited (lane 4). However, emission bands of high-molecular-weight structures could be observed in lanes 5–10, indicating that higher the ratio of the initiator to hairpins, lower the molecular weight of the HCR product was. A 1:10 ratio of initiator to hairpins triggered the longest hybridization chain, reaching a length of 2 kb. Ratios of 1.5:10 and 2:10 are similar, triggering a longer length of products, which is greater than 1.5 kb and shorter than 2 kb. The 1:10 ratio, corresponding to 100 nM  $S_3$ ,  $1\ \mu\text{M}$   $H_1$  and  $1\ \mu\text{M}$   $H_2$  was optimal. However, the absorbance ratio at 450 nm was reduced from 100 to 200 nM of  $S_3$  and slightly went up at higher concentrations (Fig. 4B), indicating that 200 nM of  $S_3$  (corresponding to  $1\ \mu\text{M}$   $H_1$  and  $H_2$ ) was optimal. Comprehensively, 200 nM of  $S_3$  was selected, considering the ideal signal amplification effect, the obvious signal report and no false positive results. Regarding the concentration of SA-HRP (Fig. 4C), the absorbance ratio at 450 nm was reduced until a stable region was achieved when the concentration of SA-HRP was denser than  $500\ \text{ng}/\text{mL}$ , demonstrating that the optimal dosage was  $500\ \text{ng}/\text{mL}$  in the absence of dissipation.

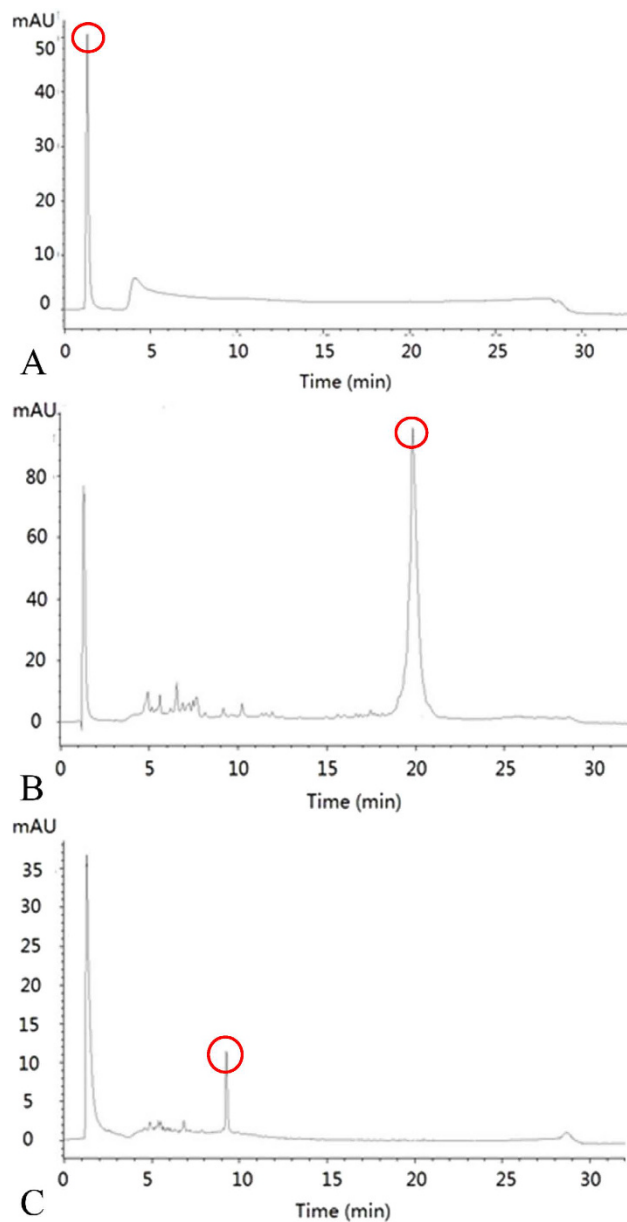


**Figure 3. Characterization of Chromatographic Behavior of  $\text{Cu}^{2+}$ -dependent DNAzyme on a DNA-NPR Column.** (A) Characterization of chromatographic behavior for the negative control of the reaction buffer on a DNA-NPR Column. (B) Characterization of chromatographic behavior for the non-dissected  $\text{Cu}^{2+}$ -dependent DNAzyme on a DNA-NPR Column. (C) Characterization of chromatographic behavior for  $\text{Cu}^{2+}$  (1 mM) cleavage of the  $\text{Cu}^{2+}$ -dependent DNAzyme on a DNA-NPR Column.

**Characterization of HCR-based HRP concatemers.** HCR products, serving as a typical non-enzymatic signal amplification element, were inspected by agarose gel electrophoresis as shown in Fig. 4A. The emission band demonstrate that HCR products were successfully formed. And the length of HCR products showed a  $S_3$  dose-response effect. When adding SA-HRP into biotinylated HCR nanostructures, an expected color change was appeared. It further confirmed that HCR-based HRP concatemers were successfully fabricated. The color change was attributed to HCR-based HRP complex could catalyze chromogen to produce chromogenic reaction. The detail color image were showed in Fig. S1. Then, transmission electron microscope (TEM) was further employed to observe the morphology of the assembled HCR-based HRP concatemers. As shown in Fig. 5A, morphology with helical concatemers was observed. The result suggested the successful formation of the HCR-based HRP concatemers. In addition, a comparison study with and without HCR-HRP have been conducted to give further validation. As shown in Fig. 5B,  $\text{OD}_{450}$  of the HCR-based system was obviously higher than that of the non-HCR system, and the sensitivity was noticeably improved, clearly indicating that the signal amplification effect of HCR process was significant, which was at least 4-fold greater than that in the non-HCR method.



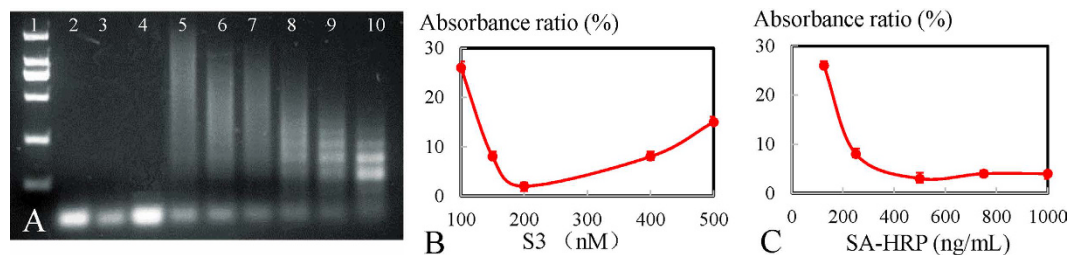


**Figure 4. Optimization of HCR-based HRP concatemers.** (A) EB-stained agarose gel electrophoresis demonstrated  $S_3$ -initiated HCR: lane 1, 2000-bp marker from top to bottom was 2000, 1000, 750, 500, 250, and 100 bp; Lane 2,  $1.0 \mu\text{M}$   $H_1$ ; Lane 3,  $1.0 \mu\text{M}$   $H_2$ ; Lane 4, mixture of  $1.0 \mu\text{M}$   $H_1$  and  $H_2$ ; Lanes 5–10, the presence of  $S_3$  (100 nM, 150 nM, 200 nM, 400 nM, 500 nM, and 600 nM) with a mixture of  $H_1$  and  $H_2$ . HCR time: 1 h. (B) Absorbance ratio (%) of the turn-off sensor with different concentrations of  $S_3$  (nM). The concentrations from the left are 100, 150, 200, 400, and 500 nM. (C) Absorbance ratio (%) of the turn-off sensor with different concentrations of SA-HRP (ng/mL). The concentrations from the left are 125, 250, 500, 750, and 1000 ng/mL. Error bars represent standard deviation ( $N = 3$ ).

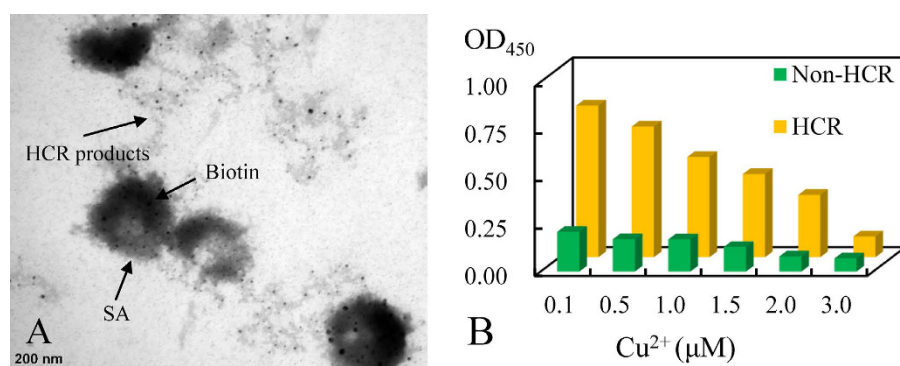


**Figure 5. The characterization of HCR-based HRP concatemers.** (A) Transmission electron microscope (TEM) of HCR-based HRP concatemers. (B) Comparison of  $OD_{450}$  with different concentrations of  $\text{Cu}^{2+}$  ( $\mu\text{M}$ ) between with and without HCR-HRP. Experimental conditions of HCR: SA,  $S_1$ ,  $S_2$ ,  $S_3$ ,  $H_1/H_2$  and SA-HRP were  $2 \mu\text{g}/\text{mL}$ , 120 nM, 120 nM, 200 nM,  $1 \mu\text{M}/1 \mu\text{M}$  and 500 ng/mL, respectively; Experimental conditions of Non-HCR: SA, 5', 3'-Biotin- $S_1$ ,  $S_2$ , and SA-HRP were  $2 \mu\text{g}/\text{mL}$ , 120 nM, 120 nM and 500 ng/mL, respectively. The detection procedure was carried out as described in the Experimental section.

**Optimization of  $\text{Cu}^{2+}$ -mediated cleavage.** Referring to the literature, a suitable dosage of ascorbate could apparently promote  $\text{Cu}^{2+}$ -mediated cleavage of specific DNAzyme in slicing buffer (1.5 M NaCl, 50 mM HEPES, pH 7.0)<sup>42</sup>. Therefore, the influence of different concentrations of ascorbate ranging from 1 to  $200 \mu\text{M}$  on visual readout was studied. As shown in Fig. 6A, the absorbance ratio at 450 nm was reduced and then increased at the concentration of  $50 \mu\text{M}$  ascorbate. These results indicate that concentrations of ascorbate less than  $50 \mu\text{M}$  enhanced the cleavage reaction, whereas concentrations greater than  $50 \mu\text{M}$  suppressed the reaction. We concluded that  $50 \mu\text{M}$  ascorbate in the slicing buffer was the ideal dosage, and this finding was consistent with Liu's results<sup>42</sup>.

To promote our  $\text{Cu}^{2+}$  turn-off sensor for on-site rapid detection, the time of  $\text{Cu}^{2+}$ -mediated cleavage was researched. As shown in Fig. 6B, the following equation was used to characterize the cleavage efficiency:  $\Delta OD_{450} (\%) = [OD_{450} (\text{negative control}) - OD_{450} (\text{sample})] / OD_{450} (\text{negative control}) \times 100\%$ <sup>7</sup>. The curve of cleavage efficiency rapidly ascended, reaching a plateau after more than 5 min. Three minutes after the addition of  $\text{Cu}^{2+}$  samples, the cleavage efficiency was greater than 80%. After 5 min, the efficiency reached 92%. Given that the immobilized  $\text{Cu}^{2+}$ -dependent DNAzyme coupled with HCR-based HRP concatemers was prepared on the surface in advance, the actual reaction time after  $\text{Cu}^{2+}$  sample introduction was in 5 min, indicating great promise for on-site rapid testing.

**Detection performance of the  $\text{Cu}^{2+}$  biosensor.** As shown in Fig. 7A, given that the  $\text{Cu}^{2+}$ -dependent DNAzyme was sensitive to the target ion when the concentration of  $\text{Cu}^{2+}$  present in samples increased from 0 nM to  $100 \mu\text{M}$ , the final visual readout of the  $\text{Cu}^{2+}$  turn-off sensor decreased accordingly until reaching a plateau. The calibration curve was monitored by optical density at 450 nm with corresponding  $\text{Cu}^{2+}$  concentrations within the range of 50 nM to  $3 \mu\text{M}$ . The linear regression equation was  $OD_{450} = -0.2376 \times [c (\text{Cu}^{2+})] + 0.8068$  ( $R^2 = 0.9933$ ), with the detection limit (LOD) of 8 nM according to  $3\sigma$  rule [mean absorbance of blank +  $3\sigma$  (standard deviation of the blank)]. According to the regulations introduced by the Chinese Ministry of Health, US EPA and WHO, the maximum permitted levels of  $\text{Cu}^{2+}$  in drinking water are  $15 \mu\text{M}$ ,  $20 \mu\text{M}$  and  $31 \mu\text{M}$ , respectively, and this

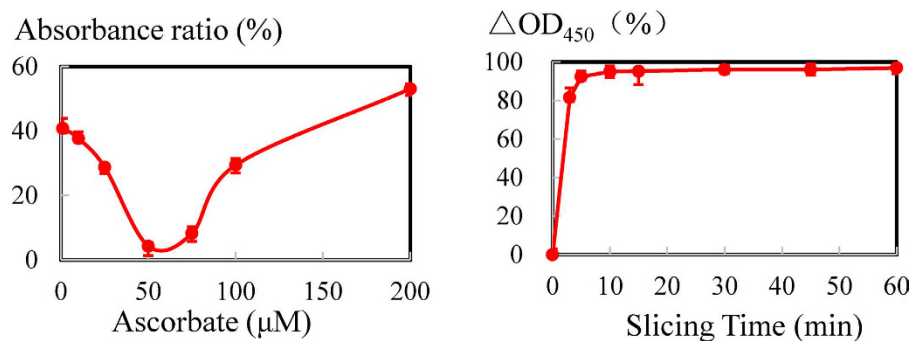


**Figure 6. Optimization of Cu<sup>2+</sup>-mediated cleavage.** (A) Absorbance ratio (%) of the turn-off sensor with different concentrations of ascorbate (μM). The ascorbate concentrations from the left are 1, 10, 25, 50, 75, 100, and 200 μM. (B) Absorbance ratio (%) of the turn-off sensor with the time of Cu<sup>2+</sup>-mediated cleavage (min). The time intervals from the left are 0, 3, 5, 10, 15, 30, 45 and 60 min. Error bars represent standard deviation (N=3).

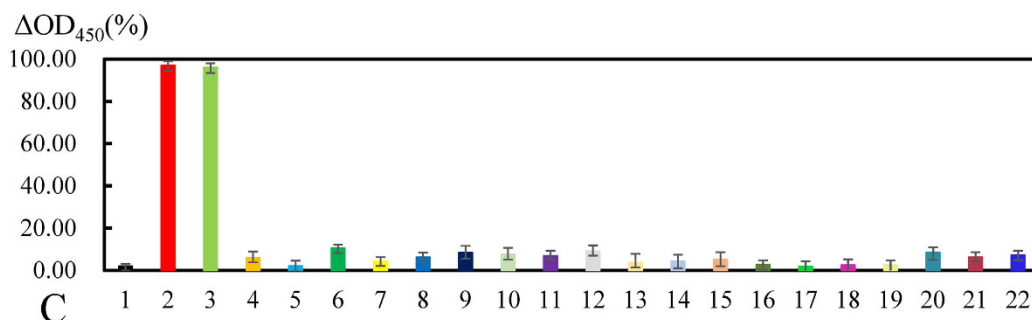
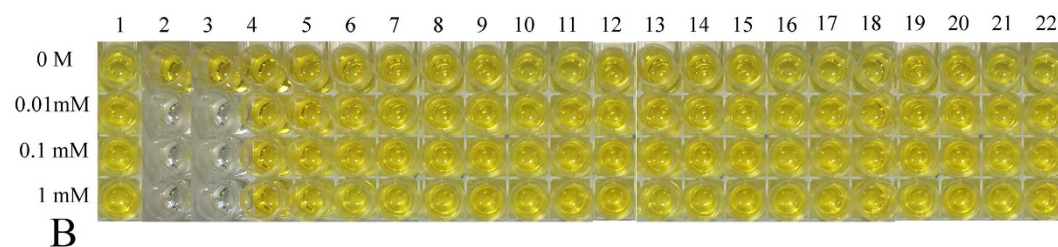
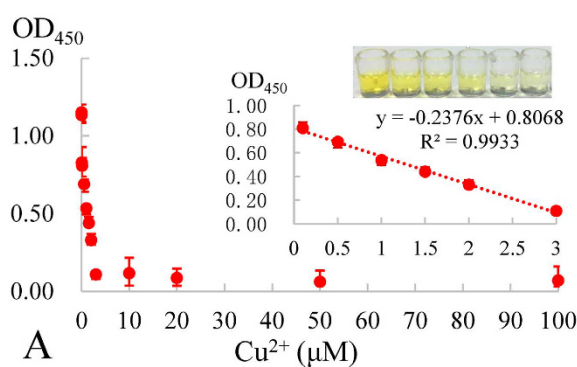


**Figure 7. Calibration curve and selectivity of the sensor.** (A) Calibration curve for colorimetric determinations of different concentrations of Cu<sup>2+</sup> by the turn-off sensor. Inset: Calibration plot and color change of Cu<sup>2+</sup> concentration vs. absorbance signal in the range from 0.05 to 3 μM. The dotted line represents the linear fit to the data. Error bars represent standard deviation (N=3). The chromogenic results (B) and OD<sub>450</sub> (C) of the Cu<sup>2+</sup> turn-off sensor before and 5 min after the addition of different metal ions of definite concentrations. Error bars represent standard deviation (N=3).

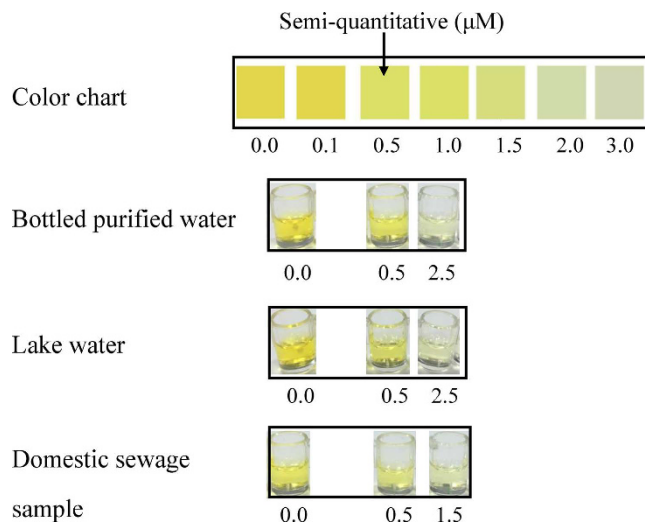


**Figure 8.** Color chart and experimental images of real sample from bottled purified water, Lake water and Domestic sewage sample.

detection limit is much lower than the regulated level. Moreover, the analytical performances of different optical DNAzyme-based assays developed for  $\text{Cu}^{2+}$  analysis are summarized, and the sensitivity of this proposed method is competitive compared with these techniques (Table S1).

The specificity of the  $\text{Cu}^{2+}$  turn-off sensor was evaluated by challenging the system against other metal ions, including  $\text{Co}^{2+}$ ,  $\text{Ti}^{2+}$ ,  $\text{Fe}^{2+}$ ,  $\text{Fe}^{3+}$ ,  $\text{Mn}^{2+}$ ,  $\text{Ca}^{2+}$ ,  $\text{Ni}^{2+}$ ,  $\text{Mg}^{2+}$ ,  $\text{Zn}^{2+}$ ,  $\text{Cd}^{2+}$ ,  $\text{Pb}^{2+}$ ,  $\text{Hg}^{2+}$ ,  $\text{Ba}^{2+}$ ,  $\text{Sr}^{2+}$ ,  $\text{UO}_2^{2+}$ ,  $\text{Eu}^{3+}$ ,  $\text{Tb}^{2+}$ ,  $\text{Ag}^+$ ,  $\text{Al}^{3+}$  and mixed ions. To evaluate the selectivity more accurately and more comprehensively, each metal ion mentioned above was analyzed at three different concentrations of  $10\ \mu\text{M}$ ,  $100\ \mu\text{M}$  and  $1\ \text{mM}$ . As indicated in Fig. 7B and C, in contrast to the significant response of  $\text{Cu}^{2+}$  ion, other metal ions exhibited minimal interference with  $\text{Cu}^{2+}$  detection. Hence, the results exhibited high selectivity toward  $\text{Cu}^{2+}$  compared with other test metal ions given the specific function of the  $\text{Cu}^{2+}$ -dependent DNAzyme.

**Determination of  $\text{Cu}^{2+}$  in water samples.** To further elucidate the analytical reliability and applicable potential of the  $\text{Cu}^{2+}$  turn-off sensor for testing real samples, three different water samples were monitored by using our developed  $\text{Cu}^{2+}$  sensor and ICP-MS. As shown in Fig. 8, a color chart was designed to assist the qualitative analysis and semi-quantitative LOD of  $0.5\ \mu\text{M}$  was clearly visualized by the naked eye.  $0.5\ \mu\text{M}$ ,  $1.5\ \mu\text{M}$  and  $2.5\ \mu\text{M}$  of  $\text{Cu}^{2+}$  could be inspected by the naked eye semi-quantitatively. Therefore, more than  $0.5\ \mu\text{M}$  of  $\text{Cu}^{2+}$  could be inspected by the naked eye. In addition, the detection performance by our strategy for the water samples spiked with  $\text{Cu}^{2+}$  was compared with reference values obtained from ICP-MS, presented in Table S2. Bottled purified water samples, which were considered to contain fewer impurities, exhibited the best recovery results both in the case of low and high  $\text{Cu}^{2+}$  concentrations. Moreover, due to the presence of various mineral components, the detection results obtained from the lake water sample were slightly increased compared with bottled purified water samples. In contrast, the detection results of the water sample from domestic sewage were considerably increased compared with the spiked amount of the  $\text{Cu}^{2+}$  standard mainly due to the inherent  $\text{Cu}^{2+}$  residual in domestic sewage. In general, the detection results were similar between our strategy and ICP-MS in samples at different  $\text{Cu}^{2+}$  concentrations and the developed  $\text{Cu}^{2+}$  turn-off sensor exhibited satisfactory accuracy for  $\text{Cu}^{2+}$  detection in real water samples.

## Conclusion

In conclusion, we constructed a rapid and visual turn-off sensor for  $\text{Cu}^{2+}$  detection, displaying several excellent features: (1) *Turn-off* type. The detection unit was composed of HCR-based HRP concatemers cross-linked with the substrate strand of  $\text{Cu}^{2+}$ -dependent DNAzyme via Watson-Crick base pairing. Upon  $\text{Cu}^{2+}$  addition,  $\text{Cu}^{2+}$ -dependent DNAzyme was irreversibly cleaved, bringing about dramatic decline of the signal output. Thus, the turn-off sensor could effectively get over false positives that interfere with the results. (2) *Visualization*. As the signal amplifier and signal report element, HCR-based HRP concatemers could catalyze hydrogen peroxide ( $\text{H}_2\text{O}_2$ ) via TMB, generating obvious green color and turning yellow after sulfuric acid termination with optical absorption at  $450\ \text{nm}$ . The signal output could be semi-quantitatively observed by the naked eye with the minimum target of  $500\ \text{nM}$  and quantitatively monitored by a portable spectrophotometer with the LOD of  $8\ \text{nM}$ , demonstrating immense potential for on-site detection. (3) *Sensitivity, Selectivity and anti-interference*. The turn-off sensor possesses outstanding sensitivity, selectivity and anti-interference, exhibiting a linear calibration from  $0.05$  to  $3\ \mu\text{M}$  with a detection limit of  $8\ \text{nM}$  and displaying remarkable applicability for monitoring  $\text{Cu}^{2+}$  in real water samples, by virtue of the specificity of DNAzyme and the signal amplification of HCR-based HRP concatemers. (4) *Rapidity*. Given that the immobilized  $\text{Cu}^{2+}$ -dependent DNAzyme coupled with HCR-based HRP concatemers was prepared on the surface in advance, the actual reaction time after the  $\text{Cu}^{2+}$  sample introduction was  $5\ \text{min}$ , indicating great promise for on-site rapid testing.



## References

- Fu, L. *et al.* Portable and quantitative monitoring of heavy metal ions using DNAzyme-capped mesoporous silica nanoparticles with a glucometer readout. *J. Mater. Chem. B* **1**, 6123–6128 (2013).
- Gumpu, M. B., Sethuraman, S., Krishnan, U. M. & Rayappan, J. B. B. A review on detection of heavy metal ions in water—An electrochemical approach. *Sens. Actuators, B* **213**, 515–533 (2015).
- Barnham, K. J. & Bush, A. I. Metals in Alzheimer's and Parkinson's diseases. *Curr. Opin. Chem. Biol.* **12**, 222–228 (2008).
- Festa, R. A. & Thiele, D. J. Copper: an essential metal in biology. *Curr. Biol.* **21**, R877–R883 (2011).
- Mihai, M., Bunia, I., Doroftei, F., Varganici, C. D. & Simionescu, B. C. Highly Efficient Copper (II) Ion Sorbents Obtained by Calcium Carbonate Mineralization on Functionalized Cross-Linked Copolymers. *Chem.-Eur. J.* **21**, 5220–5230 (2015).
- Szpunar, J. *et al.* Validation of the determination of copper and zinc in blood plasma and urine by ICP-MS with cross-flow and direct injection nebulization. *Talanta* **44**, 1389–1396 (1997).
- Seok, Y., Byun, J.-Y., Shim, W.-B. & Kim, M.-G. A structure-switchable aptasensor for aflatoxin B1 detection based on assembly of an aptamer/split DNAzyme. *Anal. Chim. Acta* **886**, 182–187 (2015).
- Chen, Y. *et al.* DNAzyme-based biosensor for Cu<sup>2+</sup> ion by combining hybridization chain reaction with fluorescence resonance energy transfer technique. *Talanta* **155**, 245–249 (2016).
- Zhu, Y., Inagaki, K. & Chiba, K. Determination of Fe, Cu, Ni, and Zn in seawater by ID-ICP-MS after preconcentration using a syringe-driven chelating column. *J. Anal. At. Spectrom.* **24**, 1179–1183 (2009).
- Pourreza, N. & Hoveizavi, R. Simultaneous preconcentration of Cu, Fe and Pb as methylthymol blue complexes on naphthalene adsorbent and flame atomic absorption determination. *Anal. Chim. Acta* **549**, 124–128 (2005).
- Atanassova, D., Stefanova, V. & Russeva, E. Co-precipitative pre-concentration with sodium diethyldithiocarbamate and ICP-AES determination of Se, Cu, Pb, Zn, Fe, Co, Ni, Mn, Cr and Cd in water. *Talanta* **47**, 1237–1243 (1998).
- Chaiyoo, S., Chailapakul, O., Sakai, T., Teshima, N. & Siangproh, W. Highly sensitive determination of trace copper in food by adsorptive stripping voltammetry in the presence of 1, 10-phenanthroline. *Talanta* **108**, 1–6 (2013).
- Lan, T. & Lu, Y. In *Interplay between Metal Ions and Nucleic Acids* 217–248 (Springer, 2012).
- Li, H., Huang, X.-X., Kong, D.-M., Shen, H.-X. & Liu, Y. Ultrasensitive, high temperature and ionic strength variation-tolerant Cu<sup>2+</sup> fluorescent sensor based on reconstructed Cu<sup>2+</sup>-dependent DNAzyme/substrate complex. *Biosens. Bioelectron.* **42**, 225–228 (2013).
- Li, H. *et al.* HCR-stimulated formation of DNAzyme concatamers on gold nanoparticle for ultrasensitive impedimetric immunoassay. *Biosens. Bioelectron.* **68**, 487–493 (2015).
- Xu, M., Gao, Z., Wei, Q., Chen, G. & Tang, D. Hemin/G-quadruplex-based DNAzyme concatamers for *in situ* amplified impedimetric sensing of copper(II) ion coupling with DNAzyme-catalyzed precipitation strategy. *Biosens. Bioelectron.* **74**, 1–7 (2015).
- Ge, Z. *et al.* Hybridization chain reaction amplification of microRNA detection with a tetrahedral DNA nanostructure-based electrochemical biosensor. *Anal. Chem.* **86**, 2124–2130 (2014).
- Fu, X., Huang, R., Wang, J. & Chang, B. Sensitive electrochemical immunoassay of a biomarker based on biotin-avidin conjugated DNAzyme concatamer with signal tagging. *Rsc Adv.* **3**, 13451–13456 (2013).
- Liu, Z. *et al.* Randomly arrayed G-quadruplexes for label-free and real-time assay of enzyme activity. *Chem. Commun.* **50**, 6875–6878 (2014).
- Saran, R. & Liu, J. A Silver DNAzyme. *Anal. Chem.* **88**, 4014–4020 (2016).
- Torabi, S. F. *et al.* *In vitro* selection of a sodium-specific DNAzyme and its application in intracellular sensing. *PNAS* **112**, 5903–5908 (2015).
- Zhou, W., Saran, R., Chen, Q., Ding, J. & Liu, J. A New Na<sup>+</sup>-Dependent RNA-Cleaving DNAzyme with over 1000-fold Rate Acceleration by Ethanol. *Chembiochem* **17**, 159–163 (2016).
- Carmi, N., Balkhi, S. R. & Breaker, R. R. Cleaving DNA with DNA. *PNAS* **95**, 2233–2237 (1998).
- Carmi, N. & Breaker, R. R. Characterization of a DNA-cleaving deoxyribozyme. *Bioorg. Med. Chem.* **9**, 2589–2600 (2001).
- Huang, P. J. & Liu, J. An Ultrasensitive Light-up Cu<sup>2+</sup> Biosensor Using a New DNAzyme Cleaving a Phosphorothioate Modified Substrate. *Anal. Chem.* **88**, 3341–3347 (2016).
- Li, W. *et al.* Detection of lead (II) ions with a DNAzyme and isothermal strand displacement signal amplification. *Biosens. Bioelectron.* **53**, 245–249 (2014).
- Pelossof, G., Tel-Vered, R. & Willner, I. Amplified surface plasmon resonance and electrochemical detection of Pb<sup>2+</sup> ions using the Pb<sup>2+</sup>-dependent DNAzyme and hemin/G-quadruplex as a label. *Anal. Chem.* **84**, 3703–3709 (2012).
- Yuan, B.-F., Xue, Y., Luo, M., Hao, Y.-H. & Tan, Z. Two DNAzymes targeting the telomerase mRNA with large difference in Mg<sup>2+</sup> concentration for maximal catalytic activity. *Int. J. Biochem. Cell Biol.* **39**, 1119–1129 (2007).
- Lu, C.-H., Wang, F. & Willner, I. Zn<sup>2+</sup>-ligation DNAzyme-driven enzymatic and nonenzymatic cascades for the amplified detection of DNA. *J. Am. Chem. Soc.* **134**, 10651–10658 (2012).
- Nelson, K. E., Bruesehoff, P. J. & Lu, Y. *In vitro* selection of high temperature Zn<sup>2+</sup>-dependent DNAzymes. *J. Mol. Evol.* **61**, 216–225 (2005).
- Zhou, W., Zhang, Y., Ding, J. & Liu, J. *In Vitro* Selection in Serum: RNA-Cleaving DNAzymes for Measuring Ca<sup>2+</sup> and Mg<sup>2+</sup>. *ACS Sensors* **1**, 600–606 (2016).
- Zhou, W., Chen, Q., Huang, P. J., Ding, J. & Liu, J. DNAzyme Hybridization, Cleavage, Degradation and Sensing in Undiluted Human Blood Serum. *Anal. Chem.* **87**, 4001–4007 (2015).
- Huang, P. J. & Liu, J. Rational evolution of Cd<sup>2+</sup>-specific DNAzymes with phosphorothioate modified cleavage junction and Cd<sup>2+</sup> sensing. *Nucleic Acids Res.* **43**, 6125–6133 (2015).
- Lee, J. H., Wang, Z., Liu, J. & Lu, Y. Highly sensitive and selective colorimetric sensors for uranyl (UO<sub>2</sub><sup>2+</sup>): Development and comparison of labeled and label-free DNAzyme-gold nanoparticle systems. *J. Am. Chem. Soc.* **130**, 14217–14226 (2008).
- Xue, X., Wang, F. & Liu, X. One-step, room temperature, colorimetric detection of mercury (Hg<sup>2+</sup>) using DNA/nanoparticle conjugates. *J. Am. Chem. Soc.* **130**, 3244–3245 (2008).
- Huang, P. J. J., Vazin, M. & Liu, J. Desulfurization Activated Phosphorothioate DNAzyme for the Detection of Thallium. *Anal. Chem.* **87**, 10443–10449 (2015).
- Huang, P. J. J., Lin, J., Cao, J., Vazin, M. & Liu, J. Ultrasensitive DNAzyme Beacon for Lanthanides and Metal Speciation. *Anal. Chem.* **86**, 1816–1821 (2014).
- Huang, P. J., Vazin, M. & Liu, J. *In vitro* selection of a new lanthanide-dependent DNAzyme for ratiometric sensing lanthanides. *Anal. Chem.* **86**, 9993–9999 (2014).
- Yin, B.-C., Ye, B.-C., Tan, W., Wang, H. & Xie, C.-C. An allosteric dual-DNAzyme unimolecular probe for colorimetric detection of copper (II). *J. Am. Chem. Soc.* **131**, 14624–14625 (2009).
- Li, J., Zheng, W., Kwon, A. H. & Lu, Y. *In vitro* selection and characterization of a highly efficient Zn (II)-dependent RNA-cleaving deoxyribozyme. *Nucleic Acids Res.* **28**, 481–488 (2000).
- Kim, S. H., Kim, J. S., Park, S. M. & Chang, S.-K. Hg<sup>2+</sup>-selective OFF-ON and Cu<sup>2+</sup>-selective ON-OFF type fluoroionophore based upon cyclam. *Org. Lett.* **8**, 371–374 (2006).
- Liu, J. & Lu, Y. A DNAzyme catalytic beacon sensor for paramagnetic Cu<sup>2+</sup> ions in aqueous solution with high sensitivity and selectivity. *J. Am. Chem. Soc.* **129**, 9838–9839 (2007).

43. Li, L., Feng, J., Fan, Y. & Tang, B. Simultaneous Imaging of Zn<sup>2+</sup> and Cu<sup>2+</sup> in Living Cells Based on DNAzyme Modified Gold Nanoparticle. *Anal. Chem.* **87**, 4829–4835 (2015).
44. Wang, Y., Yang, F. & Yang, X. Label-free colorimetric biosensing of copper (II) ions with unimolecular self-cleaving deoxyribozymes and unmodified gold nanoparticle probes. *Nanotechnology* **21**, 205502 (2010).
45. Fang, Z. *et al.* Lateral flow nucleic acid biosensor for Cu<sup>2+</sup> detection in aqueous solution with high sensitivity and selectivity. *Chem. Commun.* **46**, 9043–9045 (2010).
46. Filippov, N., Lomzov, A. & Pyshnyi, D. Thermodynamic description of oligonucleotide self-association in DNA concatamer structures. *Biophysics* **54**, 280–290 (2009).
47. Tang, J. *et al.* Hemin/G-quadruplex-based DNAzyme concatamers as electrocatalysts and biolabels for amplified electrochemical immunosensing of IgG1. *Chem. Commun.* **48**, 8180–8182 (2012).
48. Liu, J. R., Chen, G. F., Shih, H. N. & Kuo, P. C. Enhanced antioxidant bioactivity of *Salvia miltiorrhiza* (Danshen) products prepared using nanotechnology. *Phytomedicine* **15**, 23–30 (2008).
49. Wilde, C. *et al.* Quantification of gene expression by combining competitive RT-PCR with HPLC analysis. *LC GC Eur.* 17–19 (2003).
50. Bouças, R. I., Trindade, E. S., Tersariol, I. L., Dietrich, C. P. & Nader, H. B. Development of an enzyme-linked immunosorbent assay (ELISA)-like fluorescence assay to investigate the interactions of glycosaminoglycans to cells. *Anal. Chim. Acta* **618**, 218–226 (2008).
51. Lee, G. U., Kidwell, D. A. & Colton, R. J. Sensing discrete streptavidin-biotin interactions with atomic force microscopy. *Langmuir* **10**, 354–357 (1994).
52. Weber, P. C., Ohlendorf, D., Wendoloski, J. & Salemme, F. Structural origins of high-affinity biotin binding to streptavidin. *Science* **243**, 85–88 (1989).
53. Zheng, J. *et al.* Universal surface-enhanced Raman scattering amplification detector for ultrasensitive detection of multiple target analytes. *Anal. Chem.* **86**, 2205–2212 (2014).

## Acknowledgements

This work was supported by National Natural Science Foundation Project of China (31671922) and Beijing Nova Program (No. xx2014B069).

## Author Contributions

W.X., Y.L. and K.H. conceived and designed the experiments. J.T. performed the experiments. L.Z. analyzed the data. W.X. and J.T. wrote the paper. K.H. and Y.L. revised the paper. All authors reviewed the manuscript.

## Additional Information

**Supplementary information** accompanies this paper at <http://www.nature.com/srep>

**Competing financial interests:** The authors declare no competing financial interests.

**How to cite this article:** Xu, W. *et al.* A rapid and visual turn-off sensor for detecting copper (II) ion based on DNAzyme coupled with HCR-based HRP concatamers. *Sci. Rep.* **7**, 43362; doi: 10.1038/srep43362 (2017).

**Publisher's note:** Springer Nature remains neutral with regard to jurisdictional claims in published maps and institutional affiliations.



This work is licensed under a Creative Commons Attribution 4.0 International License. The images or other third party material in this article are included in the article's Creative Commons license, unless indicated otherwise in the credit line; if the material is not included under the Creative Commons license, users will need to obtain permission from the license holder to reproduce the material. To view a copy of this license, visit <http://creativecommons.org/licenses/by/4.0/>

© The Author(s) 2017